Polish Journal of Medical Physics and Engineering
The Journal of Polish Society of Medical Physics
ISSN 1898-0309, doi: 10.2478/pjmpe-2025-0032

December 2025
Vol 31, Issue 4

Scientific Paper

Estimation of the radiation damage in CA1, CA2 and CA3 pyramidal and dentate granule cell neurons during proton and carbon-ion irradiation: A study with the Geant4 toolkit

Fatemeh Dolatjavid[1,ABCDEF], Bagher Farhood[2,DEF], Mohammadali Atlasi[2,ABCF], Akbar Aliasgharzadeh[1,C], Mehran Mohseni[1,C], Eman Obeidavi[1,BC], Habiballah Moradi[1,ABCDEF*]

[1]*Medical Physics, Kashan University of Medical Sciences, Kashan, Iran*
[2]*Kashan University of Medical Sciences, Kashan, Iran*
**Corresponding author: Habiballah Moradi; habibmoradi142@gmail.com*

(received 22 September 2024; revised 20 September 2025; accepted 7 October 2025)

Abstract

Introduction: Radiation damage to the central nervous system (CNS) has been a persistent problem for decades, owing to difficulties such as brain radiotherapy and astronaut radiation protection during space flight. Hippocampus is the most radiation-sensitive structure of the central nervous system. The present study aims to investigate damage induced by ^{12}C ions and proton radiation in pyramidal neurons of cornu ammonis regions and dentate granule neurons using Geant4 toolkit.

Materials and Methods: The Geant4/Geant4-DNA Monte Carlo toolkits were used to simulate the neuron shape and particle track structures. The computations were done for various energy proton beams and ^{12}C particles with different linear energy transfers from a few to hundreds of keV/μm. Damage to pyramidal and dentate granule neurons of hippocampus as well as length reduction of the dendrites were studied by the dose absorbed in dendrite and D_{TH} (dendrites threshold dose). Also, in the present study, using Spearman's correlation test, we examined the correlation between the morphological characteristics of neurons and the reduction in the length of their dendrites.

Results: According to the results obtained in this study, the apical dendrites of CA3 and the basal dendrites of CA1 were more vulnerable following proton irradiation and carbon ions with different energies under proton and carbon radiation. But, the pyramidal neurons of CA2 were more resistant to radiation than those of CA1and CA3 regions. Furthermore, the dentate granule neurons were more resistant to radiation than the pyramidal neurons. According to the results of Spearman's correlation test, there was a statistical significance correlation (p-value< 0.05) between some of the morphological characteristics of neurons and the reduction in the length of their dendrites.

Conclusion: The results indicate that the neuron morphology is an important factor determining the accumulation of absorbed dose and length reduction of neurons. By evaluating the neurons with different morphology from the hippocampus, it was found that the dentate granule and pyramidal neurons had different vulnerabilities to radiation. The pyramidal neurons with less densely packed are more resistant to radiation.

Keywords: Geant4-DNA; Neurons; Proton therapy; Carbon ion radiotherapy; Radiation damage

Introduction

Recent technological advances in accelerator engineering, treatment planning, beam delivery, and tumor visualization have accelerated the process of moving particle radiation therapy from the laboratory to the clinic[1]. Nowadays, the use of proton radiation and heavy particle ions is considered as one of the treatment modalities for brain tumors that have distinct advantages over conventional radiotherapy. This relates to its ability to carry the high-dose treatment area to the tumor volume and therefore minimizing radiation dose to surrounding normal tissue[2]. However, extending the use of hadron therapy in the treatment of brain tumors raises concerns for the normal functioning of the brain after exposure to radiation.

Irradiation of heavy charged particles is known to cause a variety of neurological disorders in the CNS, resulting in various behavioral and cognitive impairments[3,4]. On the other hand, protons and high-charge (Z) and energy (E) (HZE) par-

Authors' contribution: A – Research concept and design, B – Collection and/or assembly of data, C – Data analysis and interpretation, D – Writing the article, E – Critical revision of the article, F – Final approval of the article.

ticles in space radiation (such as galactic cosmic rays and solar particle events) are as a limiting factor for space travel to other planets, which is considered as another potential risk factor for CNS dysfunction[5]. Early adverse effects include short-term memory impairment, reduced motor function, and behavioral changes that occur several months after irradiation. Additionally, late CNS alterations can appear as a variety of neurological disorders with symptoms consistent with accelerated aging, Alzheimer's disease and other cognitive impairments[6]. Cognitive dysfunction associated with cancer treatment has been linked to several factors, one of which is changes in the dendritic morphology of neuronal cells. Changes in dendritic geometry and branching patterns are often followed by deficiencies in learning and memory[7].

Experimental studies of possible damage mechanisms, causing the degradation of neuron morphology following low or high LET radiation, are extremely sparse[8]. The effects, therefore, cannot be completely understood without examining the earliest stages of radiation injury to individual neurons. Most experimental studies compared the vulnerability of dentate granule and CA1 pyramidal neurons of the hippocampus to damage such as radiation[9]. According to experimental studies, the vulnerability of different areas of the hippocampus cornu ammonis (CA) to injuries such as radiation is different from each other[10-14]. On the other hand, the apical and basal dendritic tree domains of pyramidal neurons have different dendritic arborization patterns, that each one were investigated separately because the synaptic input, excitability and modulation of apical and basal dendrites are different[15].

Monte Carlo techniques are efficiently used to perform detailed modeling of the stochastic energy depositions within the trajectory of the incident particle and all secondary low energy particles[16]. One of the most suitable tools for the simulation of radiation transport inside and outside neural cells is the general-purpose GEANT4 Monte Carlo toolkit, which is used in a wide range of applications, including particle physics[41] Several simulation studies have investigated the radiation damage to nervous system by using Monte Carlo processes of the Geant4-DNA toolkit. The aim of these studies was to design optimal model for realistic neuron morphology in hippocampus[5,6,18].

Hippocampus is the most radiation-sensitive structure of the central nervous system. Pyramidal and dentate granule neurons are numerically the most abundant excitatory cell types in hippocampus. Dentate granule cells are in dentate gyrus region (DG) and pyramidal cells are in CA region (CA1,CA2 and CA3)[18]. In the current study, the radiation damages induced in CA1, CA2 and CA3 pyramidal and dentate granule cell neurons during proton irradiation and carbon ions were estimated by investigating the length reduction and absorption dose of basal and apical dendrites of pyramidal and dentate granules neurons. Of note, one of the destructive effects of radiation on the central nervous system is to reduce the length of dendrites and the reduction in total dendritic length is defined as morphometric parameter to measure changes in neuron morphology[19].

Methods and Materials

Simulation of neural cell morphology

A neuron is made up of the soma, axon, and dendrites. The soma is the body of the neuron. The axon is responsible for carrying nerve signal away from the soma. The dendrites form a complicated dendritic tree and function as signal receivers[6]. There are two major groups of neuronal cells found in the hippocampus: pyramidal and dentate granule cells. Pyramidal neurons have a pyramidal-shaped soma. CA3 and CA2 pyramidal cells have wider cell bodies (approximately 25 μm diameter) than CA1 pyramidal cells (approximately 15 μm diameter). Each cell's apex and base produce separate multibranching dendritic trees. The axon arises from the cell's base, and the individual dendritic trees are referred to as apical and basilar dendrites, with each cell having one or two apical dendrites and many basilar dendrites. The apical dendritic trees radiate toward the middle of the C-shaped semicircle of cells. The basilar dendrites extend in the opposite direction. Dentate gyrus granule cells have small spherical or ovoid-shaped cell bodies (approximately 8-15 μm diameter) and are oriented in the same direction[20].

Radiobiology software ''NEURON", designed in 2016 as a subset of the GEANT4-DNA code, provides simulations of different types of neurons. The NEURON's source code is written in C++, and it contains classes that implement joining morphological points, geometrical transformations, rotations, volume and overall dimensions of the neuron, etc. The user loads a standardized SWC file of a neuron and produces a bounding volume and a homogeneous spherical medium with dimensions automatically extrapolated using the SWC file representing 3D coordinates of a neuron morphology before computing. The neural cell volume and the bounding volume are both filled with liquid water in the homogeneous medium. The user enables to modify the physical and chemical processes in the simulated media via simple UI commands, such as G4EmLivermorePhysics (compressed) or G4EmDNAPhysics (discrete) for all the medium, or a combination of compressed and discrete processes outside and inside the neuron structure[21]. The geometry of the neurons used in this code has been generated using morphological information from experimental data. In the present study, we have chosen to focus on modeling select subsets of hippocampal excitatory neurons. We select 15 pyramidal neurons from CA1, CA2, and CA3 regions as well as 5 dentate granule neurons from the dentate gyrus area of rat hippocampus were considered to simulate radiation damage induced by proton irradiation and heavy particles of carbon ion beams. The morphology of neuron is SWC format file which is presented to describe more precisely the geometry of the neuron created by digital tracking tools based on three-dimensional confocal microscopy images. The file was extracted from the Web site of NeuroMorpho.org which is an open-source database containing different groups of neuronal morphology information such as various organisms, different brain regions, and neuronal cell types. Information from this database was collected using morphological data extracted

Table 1. Morphological parameters of the neurons (presented in the NeuroMorpho.Org repository).

NeuroMorpho ID	Total length (μm)	Total surface (μm²)	Total volume (μm³)	Number of branches	Number of bifurcations	Overall width (μm)	Overall height (μm)	Overall depth (μm)
NMO_07546	1872.34	560.02	16729.00	36	16	137.01	643.01	37.22
NMO_11336	2101.05	26111.80	30737.90	27	11	154.44	882.33	31.00
NMO_08761	2901.10	1422.63	112.60	68	32	104.51	373.15	172.44
NMO_34267	4751.98	1343.59	30.23	83	40	201.55	561.42	140.86
NMO_35125	5418.31	4363.88	287.02	123	60	232.95	461.57	87.84
NMO_112003	5277.78	55203.20	42981.20	184	91	210.66	427.98	106.98
NMO_112015	6802.83	54209.10	40578.70	201	99	246.59	757.11	123.29
NMO_112025	3386.16	35858.20	32944.70	126	62	60.39	380.83	101.63
NMO_112031	5496.39	37207.60	20805.20	266	132	182.94	498.92	80.80
NMO_112033	4100.96	40172.80	32223.00	140	69	197.69	477.09	50.61
NMO_77023	1484.26	2331.46	291.43	17	8	174.15	224.71	115.50
NMO_79175	1926.96	7959.22	4964.35	90	42	132.86	199.51	37.63
NMO_79182	3970.40	14486.00	4372.00	49	24	6212.08	301.12	29.48
NMO_97828	5496.39	37207.60	20805.20	266	132	182.94	498.92	101.63
NMO_106009	7279.72	37101.80	16.57	119	58	236.14	669.09	156.73
NMO_07643	2388.02	10362.00	3691.67	23	11	177.38	201.35	143.16
NMO_07662	1337.44	6109.21	2278.16	19	9	138.01	170.27	43.54
NMO_07665	2590.71	10.1117	3276.39	27	13	164.05	231.51	63.32
NMO_32194	710.45	3255.33	3107.27	15	7	98.33	91.22	52.76
NMO_32217	1206.47	5707.37	4321.60	10	22	199.04	120.16	79.15

from neural cells in experimental studies. Moreover, the file contains information about the three-dimensional geometry of neurons with details of various parts of neuron. Using the data from the public depository www.neuromorpho.org, the main morphological parameters of the selected neurons are presented in **Table 1**.

Different parts of neurons were simulated using a combination of spheres and cylinders. The cell body is a combination of spheres and the dendrites are a combination of cylinders. The volumes of the simulated neurons are in the ranges of 291.433 μm³ to 128388 μm³.

Simulation of Radiation

The NEURON software can simulate and track proton and heavy-ion radiation such as carbon, ^{16}O and ^{56}Fe. In this study, NEURON software was used to determine the energy and absorbed dose of proton radiation in dentate granule and pyramidal neurons. The ''NEURON" example has been discussed in the latest Geant4 version 10.4.1.

The entrance parameters of protons and ^{12}C particle are set on the basis of the experimental data. Particle beam trajectories were produced inside the box in a direction parallel to the Z axis. The particle tracks were distributed randomly in the X-Y plane. The outlines of the parameters used in the simulations are listed in **Tables 2**, **3**, **4** and **5**. In the tables, N_{trial} (number of trials) is the number of particles traversing the water box in each trial which is calculated as follows:

$$N_{trial} = \frac{A \times D}{0.1602 \times LET} \quad (1)$$

where "$D = N_{trial} \times D_{beam}$" is the fluence dose (Gy) and "D_{beam}" is the dose per beam (Gy). When a primary particle or a secondary electron traverses a neuron, N_{target} is the cumulative number of target coincidence events. "*A*" refers to the X-Y radiation projection area (μm²) and "*LET*" demonstrates linear energy transfer of the incident particles (keV/μm).

Table 2. The physical parameters of ionizing radiations of CA1 pyramidal neurons.

Neuromorpho ID	Particle energy	LET (Kev/μm)	Dose per beam, (Gy)	Fluence dose, D (Gy)	Number of trials, N_{trial}	Number of particle coincidences, N_{target}
NMO_07546	Protons (p) 30 Mev	1.8663	1.8726×10^{-7}	1.50.1, 0.5, 1.0,	534010 ,26700805340160 ,8010250	3560 ,4177990 35529 ,53138
NMO_07546	60 MeV	1.0728	1.0764×10^{-7}	1.50.1, 0.5, 1.0,	929020 ,4645110 ,9290220 ,13935340	5987 ,30085 ,59821 ,89965
NMO_07546	100 MeV	0.7256	7.2804×10^{-8}	1.50.1, 0.5, 1.0,	1373500 ,6867700 ,1373550 ,20603260	8522 ,42188 ,84802 ,127292

tab. 2 cont.

Neuromorpho ID	Particle energy	LET (Kev/μm)	Dose per beam, (Gy)	Fluence dose, D (Gy)	Number of trials, N_{trial}	Number of particle coincidences, N_{target}
NMO_07546	Carbon ions (^{12}C) 300 MeV/u	12.624	1.2666×10^{-6}	1.50.1, 0.5, 1.0,	78950 ,394750 ,789510 ,1184270	1195 ,9541 ,12050 ,18058
NMO_07546	11.1 MeV/u	149.0	1.495×10^{-5}	1.50.1, 0.5, 1.0,	6720 ,33440 ,6680 ,100330	93 ,351 ,88 ,1058
NMO_11336	Protons (p) 30 Mev	1.8663	9.8225×10^{-8}	1.50.1, 0.5, 1.0,	1018070 ,5090350 ,101807 ,15271060	89220 ,490577 ,981990 ,1471889
NMO_11336	60 MeV	1.0728	5.646×10^{-8}	1.50.1, 0.5, 1.0,	1771160 ,8855820 ,17711650 ,26567480	166226 ,831384 ,1661402 ,249244
NMO_11336	100 MeV	0.7256	3.8189×10^{-8}	1.50.1, 0.5, 1.0,	2618500 ,13092700 ,26185550 ,39278320	229240 ,11476 ,2295084 ,3440818
NMO_11336	Carbon ions(^{12}C) 300 Mev/u	12.624	6.6441×10^{-7}	1.50.1, 0.5, 1.0,	150500 ,752540 ,1505090 ,2257640	28579 ,143550 ,288056 ,432107
NMO_11336	11.1 MeV/u	149.0	7.8421×10^{-6}	1.50.1, 0.5, 1.0,	12750 ,63750 ,127510 ,191270	541 ,2684 ,5259 ,7918
NMO_08761	Protons (p) 30 Mev	1.8663	4.3582×10^{-7}	1.50.1, 0.5, 1.0,	229450 ,1147260 ,229452 ,3441780	1303 ,6432 ,12990 ,19421
NMO_08761	60 Mev	1.0728	2.5051×10^{-7}	1.50.1, 0.5, 1.0,	399180 ,1995920 ,3991850 ,5987780	1874 ,9209 ,18329 ,27512
NMO_08761	100 Mev	0.7256	1.6944×10^{-7}	1.50.1, 0.5, 1.0,	590170 ,2950890 ,5901790 ,8852690	2282 ,11258 ,22720 ,33951
NMO_08761	Carbon ions(^{12}C) 300 Mev/u	12.624	2.948×10^{-6}	1.50.1, 0.5, 1.0,	33920 ,169600 ,339210 ,508810	634 ,3059 ,6106 ,9193
NMO_08761	11.1 Mev/u	149.0	3.4795×10^{-5}	1.50.1, 0.5, 1.0,	2870 ,14360 ,28730 ,43100	97 ,465 ,984 ,1488
NMO_34267	Proton (P) 30 Mev	1.8663	1.9082×10^{-7}	1.50.1, 0.5, 1.0,	52405 ,2620270 ,5240540 ,7860810	16290 ,8233 ,16301 ,24474
NMO_34267	60 Mev	1.0728	1.0968×10^{-7}	1.50.1, 0.5, 1.0,	911740 ,4558710 ,9117430 ,13676140	2599 ,12995 ,25995 ,39123
NMO_34267	100 Mev	0.7256	7.4186×10^{-8}	1.50.1, 0.5, 1.0,	1347900 ,6739800 ,13479630 ,20219440	3609 ,17707 ,35789 ,53981
NMO_34267	Carbon ions(^{12}C) 300 Mev/u	12.624	1.2907×10^{-6}	1.50.1, 0.5, 1.0,	77470 ,387380 ,774770 ,1162160	781 ,3943 ,7815 ,11760
NMO_34267	11.1 Mev/u	149.0	1.5234×10^{-5}	1.50.1, 0.5, 1.0,	6560 ,32820 ,65640 ,98460	93 ,478 ,960 ,1442
NMO_35125	Protons (p) 30 Mev	1.8663	2.5533×10^{-7}	1.50.1, 0.5, 1.0,	391650 ,1958250 ,3916500 ,5874750	3302 ,16498 ,32681 ,49129
NMO_35125	60 Mev	1.0728	1.4676×10^{-7}	1.50.1, 0.5, 1.0,	681380 ,3406920 ,6813840 ,10220760	4092 ,20673 ,41422 ,62282
NMO_35125	100 Mev	0.7256	9.9268×10^{-8}	1.50.1, 0.5, 1.0,	1007300 ,5036800 ,1007300 ,45110600	4867 ,24079 ,48227 ,72070
NMO_35125	Carbons ions (^{12}C) 300 Mev/u	12.624	1.7271×10^{-6}	1.50.1, 0.5, 1.0,	57900 ,289500 ,579000 ,868500	1780 ,8934 ,17581 ,26443
NMO_35125	11.1 Mev/u	149.0	2.0385×10^{-5}	1.50.1, 0.5, 1.0,	4900 ,24520 ,49050 ,73580	248 ,1210 ,2421 ,3624

Table 3. The physical parameters of ionizing radiations of CA2 pyramidal neurons.

Neuromorpho ID	Particle energy	LET Kev/μm)	Dose per beam, (Gy)	Fluence dose, D (Gy)	Number of trials, N_{trial}	Number of particle coincidences, N_{target}
NMO_112003	Protons (p) 30 Mev	1.8663	2.6347×10^{-7}	0.1,0.5,1.0,1.5	379540 ,1897740 ,3795490 ,5693240	50453 ,254085 ,508432 ,763810
NMO_112003	60 Mev	1.0728	1.5144×10^{-7}	0.1,0.5,1.0,1.5	660320 ,3301630 ,6603270 ,14644140	83203 ,415213 ,830427 ,1245722
NMO_112003	100 Mev	0.7256	1.0243×10^{-7}	0.1,0.5,1.0,1.5	976270 ,4881380 ,9762760 ,14644140	108698 ,544405 ,1088115 ,1632904
NMO_112003	Carbon ions (^{12}C) 300 Mev/u	12.624	1.7821×10^{-6}	0.1,0.5,1.0,1.5	56110 ,280560 ,561130 ,841700	15905 ,79833 ,159676 ,239148
NMO_112003	11.1 Mev/u	149.0	2.1035×10^{-5}	0.1,0.5,1.0,1.5	4750 ,23760 ,47530 ,71300	864 ,43366 ,8823 ,13261
NMO_112015	Protons (p) 30 Mev	و 1.8663	1.0714×10^{-7}	0.1,0.5,1.0,1.5	933350 ,4666790 ,9333580 ,14000370	75354 ,376470 ,752938 ,1129203
NMO_112015	60 Mev	1.0728	6.1585×10^{-8}	0.1,0.5,1.0,1.5	1623770 ,8118860 ,1627720 ,24356580	119649 ,599127 ,1198716 ,1795539

tab. 3 cont.

Neuromorpho ID	Particle energy	LET Kev/μm)	Dose per beam, (Gy)	Fluence dose, D (Gy)	Number of trials, N_{trial}	Number of particle coincidences, N_{target}
NMO_112015	100 Mev	0.725	4.1656×10^{-7}	0.1,0.5,1.0,1.5	2400610 ,12003070 ,24006140 ,36009210	153397 ,768484 ,15360634 ,2302935
NMO_112015	Carbon ions (^{12}C) 300 Mev/u	12.624	7.2473×10^{-7}	0.1,0.5,1.0,1.5	137980 ,689910 ,1379820 ,2069730	27094 ,134660 ,268589 ,403292
NMO_112015	11.1 Mev/u	149.0	8.5541×10^{-6}	0.1,0.5,1.0,1.5	11690 ,58450 ,116900 ,175350	730 ,3633 ,342 ,11011
NMO_112025	Protons (p) 30 Mev	1.8663	3.8354×10^{-7}	0.1,0.5,1.0,1.5	260720 ,1303640 ,2607280 ,3910930	51811 ,259686 ,518934 ,778618
NMO_112025	60 Mev	1.0728	2.2046×10^{-7}	0.1,0.5,1.0,1.5	453590 ,2267980 ,4535970 ,6803950	85481 ,451543 ,853313 ,1279994
NMO_112025	100 Mev	0.7256	1.4911×10^{-7}	0.1,0.5,1.0,1.5	670640 ,3353220 ,6706450 ,10059680	135831 ,565806 ,1130901 ,1697035
NMO_112025	Carbon ions (^{12}C) 300 Mev/u	12.624	2.5943×10^{-6}	0.1,0.5,1.0,1.5	38540 ,192730 ,385460 ,578190	14278 ,70893 ,141680 ,21306
NMO_112025	11.1 Mev/u	149.0	3.0621×10^{-5}	0.1,0.5,1.0,1.5	3260 ,16320 ,32650 ,48980	903 ,4594 ,9216 ,13828
NMO_112031	Protons (p) 30 Mev	1.8663	2.3845×10^{-7}	0.1,0.5,1.0,1.5	419370 ,2096870 ,4193750 ,6290620	45266 ,2268833 ,452568 ,679459
NMO_112031	Mev 60	1.0728	1.3706×10^{-7}	0.1,0.5,1.0,1.5	729600 ,3648030 ,7296070 ,1094410	69855 ,349357 ,699324 ,1049087
NMO_112031	Mev 100	0.7256	9.2708×10^{-8}	0.1,0.5,1.0,1.5 0.1,0.5,1.0,1.5	1078650 ,5393270 ,10786550 ,16179830	86502 ,432304 ,866342 ,1300301
NMO_112031	Carbon ions (^{12}C) 300 Mev/u	12.624	1.6129×10^{-6}	0.1,0.5,1.0,1.5	62000 ,310000 ,6200000 ,9300000	15011 ,75300 ,150235 ,225730
NMO_112031	11.1 Mev/u	149.0	1.9038×10^{-5}	0.1,0.5,1.0,1.5	5250 ,26260 ,52520 ,78780	889 ,4315 ,8657 ,13012
NMO_112033	Protons (p) 30 Mev	1.8663	2.8451×10^{-7}	0.1,0.5,1.0,1.5	351480 ,1754700 ,3514810 ,5272220	46481 ,231296 ,471150 ,692697
NMO_112033	60 Mev	1.0728	1.6354×10^{-7}	0.1,0.5,1.0,1.5	611470 ,3057350 ,6114710 ,9172060	75842 ,378819 ,757042 ,1135172
NMO_112033	100 Mev	0.7256	1.1061×10^{-7}	0.1,0.5,1.0,1.5	904070 ,4520380 ,9040770 ,135611160	99727 ,498076 ,994650 ,1494029
NMO_112033	Carbon ions (^{12}C) 300 Mev/u	12.624	1.9245×10^{-6}	0.1,0.5,1.0,1.5	51960 ,259800 ,519610 ,779420	14136 ,70431 ,140205 ,210024
NMO_112033	11.1 Mev/u	149.0	2.2715×10^{-5}	0.1,0.5,1.0,1.5	4400 ,22010 ,44020 ,66030	820 ,4029 ,8033 ,12099

Table 4. The physical parameters of ionizing radiations of CA3 pyramidal neurons.

Neuromorpho ID	Particle energy	LET (Kev/μm)	Dose per beam, (Gy)	Fluence dose, D (Gy)	Number of trials, N_{trial}	Number of particle coincidences, N_{target}
NMO_77023	Protons (p) 30 Mev	1.8663	8.3151×10^{-7}	0.1,0.5,1.0,1.5	120260 ,601310 ,1202630 ,1484850	2033 ,10032 ,20007 ,138220
NMO_77023	60 Mev	1.0728	4.7795×10^{-7}	0.1,0.5,1.0,1.5	209220 ,1046130 ,2092260 ,3138400	2381 ,11623 ,23114 ,34725
NMO_77023	100 Mev	0.7256	3.2328×10^{-7}	0.1,0.5,1.0,1.5	309320 ,1546640 ,3093290 ,4639940	2408 ,11949 ,23817 ,35656
NMO_77023	Carbon ions (^{12}C) 300 Mev/u	12.624	5.6244×10^{-6}	0.1,0.5,1.0,1.5	17770 ,88890 ,177790 ,266690	842 ,4393 ,8744 ,13122
NMO_77023	11.1 Mev/u	149.0	6.6386×10^{-5}	0.1,0.5,1.0,1.5	1500 ,7530 ,15060 ,22590	138 ,640 ,1314 ,1967
NMO_79175	Protons (p) 30 Mev 30 Mev	1.8663	1.0102×10^{-6}	0.1,0.5,1.0,1.5	98990 ,494950 ,989900 ,1803940	9320 ,45927 ,92070 ,29897
NMO_79175	60 Mev	1.0728	5.8069×10^{-7}	0.1,0.5,1.0,1.5	172200 ,861040 ,1722080 ,2583130	13254 ,66496 ,133764 ,200869
NMO_79175	100 Mev	0.7256	3.9277×10^{-7}	0.1,0.5,1.0,1.5	254600 ,1273000 ,2546010 ,3819020	16109 ,81125 ,162693 ,244005
NMO_79175	Carbon ions (^{12}C) 300 Mev/u	12.624	6.8334×10^{-6}	0.1,0.5,1.0,1.5	14630 ,73170 ,146340 ,219510	2768 ,14076 ,27911 ,42053
NMO_79175	11.1 Mev/u	149.0	8.0656×10^{-5}	0.1,0.5,1.0,1.5	1230 ,6190 ,12390 ,18590	248 ,1225 ,2484 ,3770
NMO_79182	Protons (p) 30 Mev 30 Mev	1.8663	4.185×10^{-7}	0.1,0.5,1.0,1.5	238940 ,1194740 ,2389480 ,3584220	20762 ,103818 ,208293 ,312208

tab. 4 cont.

Neuromorpho ID	Particle energy	LET (Kev/μm)	Dose per beam, (Gy)	Fluence dose, D (Gy)	Number of trials, N_{trial}	Number of particle coincidences, N_{target}
NMO_79182	60 Mev	1.0728	2.4055×10^{-7}	0.1,0.5,1.0,1.5	415710 ,2078560 ,4157130 ,6235700	28986 ,144871 ,290386 ,435904
NMO_79182	100 Mev	0.7256	1.6271×10^{-7}	0.1,0.5,1.0,1.5	614590 ,3072950 ,6145900 ,9218850	33778 ,3072950 ,339429 ,509095
NMO_79182	Carbon ions (^{12}C) 300 Mev/u	12.624	2.8308×10^{-6}	0.1,0.5,1.0,1.5	35320 ,176620 ,353250 ,529880	6806 ,33733 ,67482 ,101551
NMO_79182	11.1 Mev/u	149.0	3.3412×10^{-5}	0.1,0.5,1.0,1.5	2990 ,14960 ,29920 ,44890	587 ,2884 ,5805 ,8669
NMO_97828	Protons (p) 30 Mev 30 Mev	1.8663	1.3602×10^{-7}	0.1,0.5,1.0,1.5	735180 ,3675930 ,7351860 ,11027790	2283 ,11517 ,23113 ,34697
NMO_97828	60 Mev	1.0728	7.8182×10^{-8}	0.1,0.5,1.0,1.5	1279060 ,6395330 ,12790660 ,19186000	3476 ,17740 ,35822 ,52776
NMO_97828	100 Mev	0.7256	5.2881×10^{-8}	0.1,0.5,1.0,1.5	1891030 ,9455190 ,18910380 ,1630380	463 ,23289 ,46851 ,70097
NMO_97828	Carbon ions (^{12}C) 300 Mev/u	12.624	9.2003×10^{-7}	0.1,0.5,1.0,1.5	108690 ,543460 ,1086920 ,1630380	1014 ,5377 ,10624 ,15924
NMO_97828	11.1 Mev/u	149.0	1.0859×10^{-5}	0.1,0.5,1.0,1.5	9200 ,46040 ,92080 ,138130	63 ,293 ,601 ,887
NMO_106009	Protons (p) 30 Mev 30 Mev	1.8663	3.4014×10^{-7}	0.1,0.5,1.0,1.5	293990 ,1469980 ,2939960 ,11343010	5202 ,26504 ,53329 ,205847
NMO_106009	60 Mev	1.0728	1.9551×10^{-7}	0.1,0.5,1.0,1.5	511500 ,2557410 ,5114820 ,7672240	6955 ,34681 ,69571 ,104345
NMO_106009	100 Mev	0.7256	1.3224×10^{-7}	0.1,0.5,1.0,1.5	756200 ,3781000 ,7562000 ,11343010	8055 ,40901 ,82281 ,123732
NMO_106009	Carbon ions (^{12}C) 300 Mev/u	12.624	2.3008×10^{-6}	0.1,0.5,1.0,1.5	43460 ,217310 ,434630 ,651940	2164 ,11175 ,22472 ,33718
NMO_106009	11.1 Mev/u	149.0	2.7156×10^{-5}	0.1,0.5,1.0,1.5	3680 ,18410 ,36820 ,55230	286 ,1436 ,2916 ,4446

Table 5. The physical parameters of ionizing radiations of granule neurons.

Neuromorpho ID	Particle energy	LET (Kev/μm)	Dose per beam, (Gy)	Fluence dose, D (Gy)	Number of trials, N_{trial}	Number of particle coincidences, N_{target}
NMO_07643	Protons (p) 30 Mev	1.8663	6.9519×10^{-7}	0.1,0.5,1.0,1.5	143840 ,719220 ,1438450 ,2157680	8739 ,43717 ,87145 ,130639
NMO_07643	60 Mev	1.0728	3.996×10^{-7}	0.1,0.5,1.0,1.5	250250 ,1251250 ,2502500 ,375375	12328 ,62023 ,123723 ,185471
NMO_07643	100 Mev	0.7256	2.7028×10^{-7}	0.1,0.5,1.0,1.5	369980 ,1849930 ,3699860 ,5549800	14353 ,72383 ,144690 ,217279
NMO_07643	Carbon ions (^{12}C) 300 Mev/u	12.624	4.7024×10^{-6}	0.1,0.5,1.0,1.5	21260 ,106320 ,212650 ,38980	2928 ,14885 ,29743 ,44609
NMO_07643	11.1 Mev/u	149.0	5.5503×10^{-5}	0.1,0.5,1.0,1.5	1800 ,9000 ,18010 ,27020	259 ,1249 ,2606 ,3922
NMO_07662	Protons (p) 30 Mev 30 Mev	1.8663	1.1533×10^{-6}	0.1,0.5,1.0,1.5	86700 ,433530 ,867070 ,1300610	6907 ,34419 ,68905 ,103442
NMO_07662	60 Mev	1.0728	6.6292×10^{-7}	0.1,0.5,1.0,1.5	150840 ,754230 ,1508470 ,2262710	10007 ,50215 ,100174 ,150294
NMO_07662	100 Mev	0.7256	4.4839×10^{-7}	0.1,0.5,1.0,1.5	223020 ,1115100 ,2230200 ,3345300	11916 ,60249 ,120146 ,180261
NMO_07662	Carbon ions (^{12}C) 300 Mev/u	12.624	7.8011×10^{-6}	0.1,0.5,1.0,1.5	12810 ,64090 ,128180 ,192280	2040 ,10391 ,20805 ,31397
NMO_07662	11.1 Mev/u	149.0	9.2078×10^{-5}	0.1,0.5,1.0,1.5	1080 ,5430 ,10860 ,16290	185 ,929 ,1935 ,2910
NMO_07665	Protons (p) 30 Mev 30 Mev	1.8663	7.9356×10^{-7}	0.1,0.5,1.0,1.5	125540 ,627720 ,1255440 ,1883160	10577 ,52322 ,104672 ,157363
NMO_07665	60 Mev	1.0728	4.5785×10^{-7}	0.1,0.5,1.0,1.5	218410 ,1092060 ,2184120 ,3276180	14555 ,73112 ,146465 ,219592
NMO_07665	100 Mev	0.7256	3.0968×10^{-7}	0.1,0.5,1.0,1.5	322910 ,1614560 ,3229130 ,4843700	16890 ,84827 ,169941 ,254618
NMO_07665	Carbon ions (^{12}C) 300 Mev/u	12.624	5.3879×10^{-6}	0.1,0.5,1.0,1.5	18560 ,92800 ,185600 ,278400	3445 ,17125 ,34190 ,51248
NMO_07665	11.1 Mev/u	149.0	6.3594×10^{-5}	0.1,0.5,1.0,1.5	1570 ,7860 ,15720 ,23580	299 ,1597 ,3190 ,4836

tab. 5 cont.

Neuromorpho ID	Particle energy	LET (Kev/ µm)	Dose per beam, (Gy)	Fluence dose, D (Gy)	Number of trials, N_{trial}	Number of particle coincidences, N_{target}
NMO_32194	Protons (p) 30 Mev 30 Mev	1.8663	2.7226×10^{-6}	0.1,0.5,1.0,1.5	36720 ,183640 ,367290 ,550940	2885 ,14715 ,29202 ,43386
NMO_32194	60 Mev	1.0728	1.565×10^{-6}	0.1,0.5,1.0,1.5	63890 ,319480 ,638970 ,958460	4178 ,21014 ,41496 ,62280
NMO_32194	100 Mev	0.7256	1.0585×10^{-6}	0.1,0.5,1.0,1.5	94470 ,472360 ,944730 ,1417090	5097 ,25812 ,51384 ,77048
NMO_32194	Carbon ions (^{12}C) 300 Mev/u	12.624	1.8416×10^{-5}	0.1,0.5,1.0,1.5	5430 ,27150 ,54300 ,81450	795 ,4125 ,8410 ,12531
NMO_32194	11.1 Mev/u	149.0	21.737×10^{-5}	0.1,0.5,1.0,1.5	460 ,2300 ,4600 ,6900	90 ,444 ,909 ,1346
NMO_32217	Protons (p) 30 Mev 30 Mev	1.8663	1.85×10^{-6}	0.1,0.5,1.0,1.5	54050 ,270270 ,540540 ,810810	3648 ,18259 ,364569 ,55003
NMO_32217	60 Mev	1.0728	1.0634×10^{-6}	0.1,0.5,1.0,1.5	94030 ,470180 ,940370 ,1410560	5105 ,25379 ,51122 ,76544
NMO_32217	100 Mev	0.7256	7.1972×10^{-7}	0.1,0.5,1.0,1.5	139020 ,695140 ,1390290 ,2085440	6058 ,30422 ,61276 ,92076
NMO_32217	Carbon ions (^{12}C) 300 Mev/u	12.624	1.2514×10^{-5}	0.1,0.5,1.0,1.5	7990 ,39950 ,79910 ,119860	1129 ,5597 ,11177 ,16864
NMO_32217	11.1 Mev/u	149.0	1.477×10^{-5}	0.1,0.5,1.0,1.5	677 ,3385 ,6770 ,10156	1271 ,637 ,1282 ,1867

Estimation of radiation-induced length reduction of neuronal cell

Neuronal cell morphology is an important agent in estimating the energy and the dose absorbed on different parts of the cell. Dendrites are critical parts of the neuron cell and their damage leads to change in neuron morphology, causing a break in neurons connections. Due to their geometric structure, a threshold dose requires to estimate damage in dendrites. We assume that a local damage is identified as a candidate snip site based on the severity of the energy deposition (ED) to a neuronal segment[7].

A probabilistic model (described below) decides if a given site will be snipped, with larger ED having a higher probability. Both branches and their segments in the soma-to-tip direction assisted by the cut branch are snipped if a segment is determined to be snipped. If a section is determined to be snipped, all branches and their segments assisted by the cut branch in the soma-to-tip direction are removed from the original neuron. Many segments in a neuron can be calculated to be snipped, even one on the same branch at a given absorbed dose. The snipped segments closest to the soma on the tip-to-soma direction pathway decide the segments survive and where branches end. On the remaining neuron, the new total dendritic length is determined. At a given cumulative segment microscopic dose, D_{seg}, and probability of snip occurrence, P_{snip}, which is modeled by an exponential response function, snip sites on dendritic segments undergo excision processes:

$$P_{snip} = 1 - \exp\left(\frac{D_{seg}}{D_{TH}}\right) \quad (2)$$

Where D_{TH} represents the threshold dose showing that 63% of the dendrites are damaged. In this work, we considered three different values for D_{TH} (270 Gy, 350 Gy and 430 Gy) ,based on Alp et al. study[7,19].

Investigating correlation between morphology characteristics of neurons and their length reduction

Based on Spearman's correlation analysis, a statistical significant correlation was found between the morphological characteristics of pyramidal and dentate granule simulated neurons and the amount of length reduction (p-value < 0.05). In this study, due to the small number of statistical samples (the number of simulated neurons), the non-significance of correlation between the studied parameters does not mean no correlation.

Results

The effect of neuronal damage on dendritic length reduction

The reducing the length of apical and basal dendrites of pyramidal neurons and dendrites of dentate granule neurons following different energies of protons and carbon ions are shown in **Figures 1, 2, and 3**. These results have been obtained from absorbed doses in the dendrites. The dendrites length was further reduced by increasing the absorbed dose. According to **Eq. 2**, the radiation-induced damage probability increases with an increment in the dose absorbed in the dendrite. The highest reduction in dendrites was related to carbon ion beams with 11.1 MeV/u and the lowest was related to proton radiation with 100 MeV energy. Furthermore, the minimum and maximum length reduction of apical and basal dendrites of pyramidal neurons and dendrites of dentate granule neurons following different energies of protons and carbon ions are given in **Tables 6**, **7**, and **8**, respectively.

The obtained results from the length reduction of pyramidal and dentate granule neurons based on various D_{TH} values (270 Gy, 350 Gy and 430 Gy) are also shown in **Figures 4**, **5** and **6**. The findings showed that the morphometric characteristics of a neuron affect by the D_{TH} values; as for smaller D_{TH}, there were more snips and dendritic reduction was encouraged.

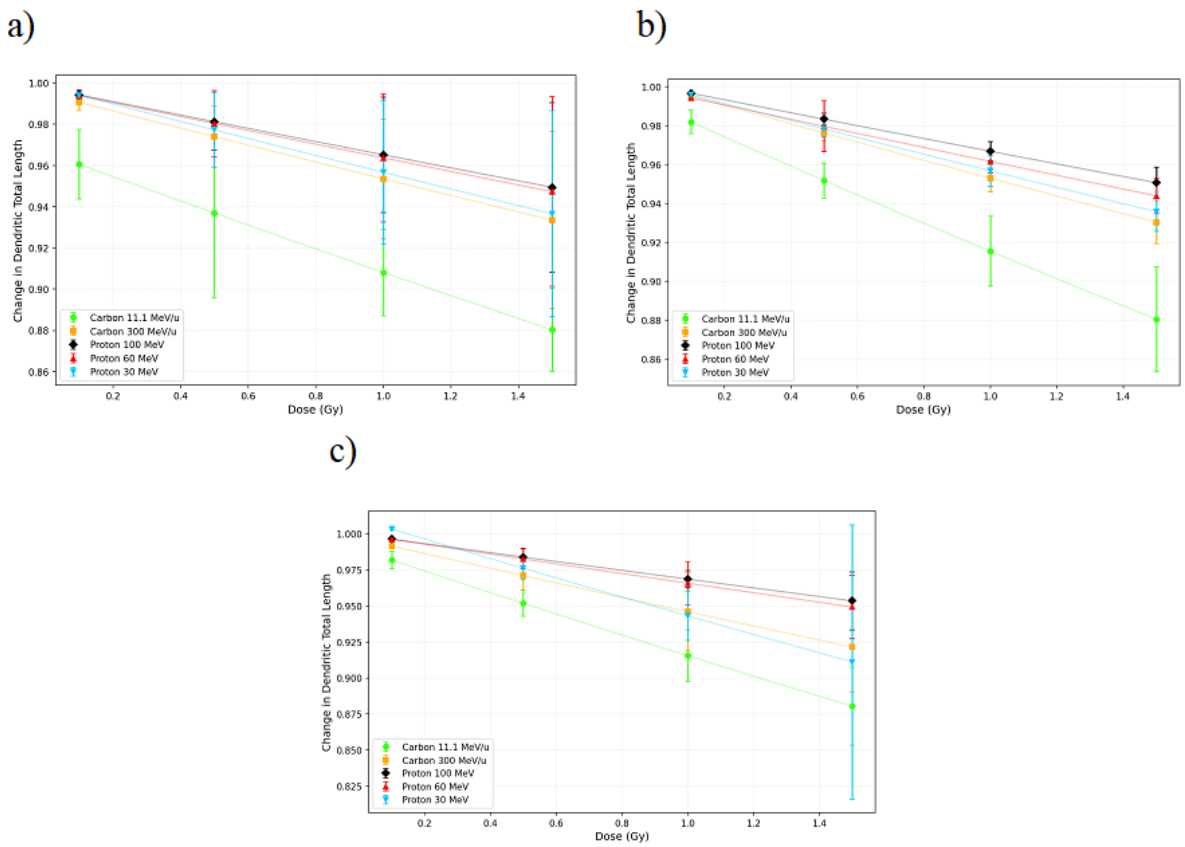

Figure 1. Dose-dependent damage induced by proton radiation and carbon ion beams on apical dendrites of CA1 (a), CA2 (b) and CA3 (c) pyramidal neurons in 270 Gy D_{TH}.

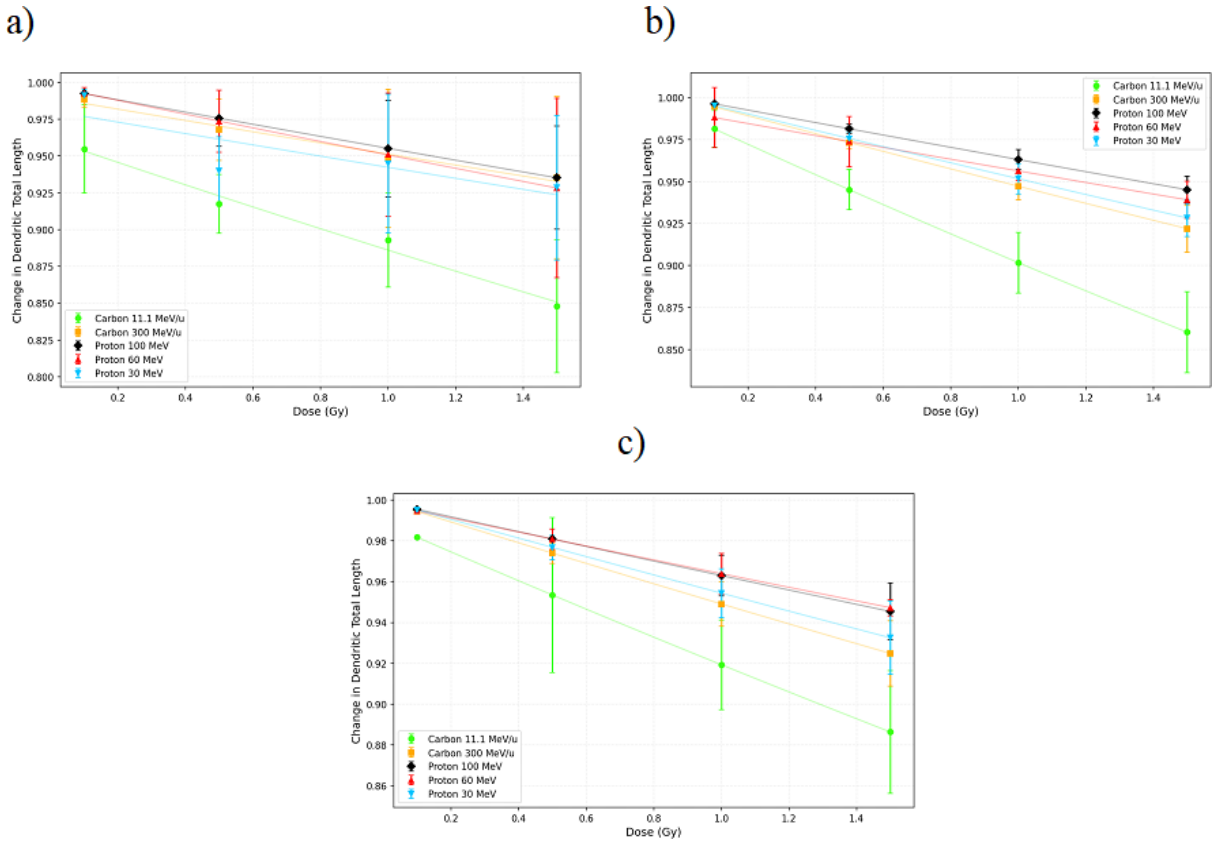

Figure 2. Dose-dependent damage induced by proton radiation and carbon ion beams on basal dendrites of CA1 (a), CA2 (b) and CA3 (c) pyramidal neurons in 270 Gy D_{TH}.

Table 6. Minimum and maximum length reduction of apical dendrites of hippocampal pyramidal neurons following proton radiation and carbon ion beams in 270 Gy D_{TH}

Particle type (energy beam)	Max reduction length (%)			Min reduction length (%)		
	CA1	CA2	CA3	CA1	CA2	CA3
Proton (30 MeV)	6.35	6.53	10.07	0.632	0.45	0.45
Proton (60 MeV)	5.3	5.58	5.09	0.626	0.38	0.38
Proton (100 MeV)	5.05	4.95	4.53	0.58	0.34	0.35
Carbon (300 MeV/u)	6.66	6.98	7.00	0.99	0.48	0.62
Carbon (11.1 MeV/u)	11.41	12.10	12.20	2.86	2.02	2.37

Table 7. Minimum and maximum length reduction of basal dendrites of hippocampal pyramidal neurons following proton radiation and carbon ion beams in 270 Gy D_{TH}

Particle type (energy beam)	Max reduction length (%)			Min reduction length (%)		
	CA1	CA2	CA3	CA1	CA2	CA3
Proton (30 MeV)	7.16	7.24	6.75	0.88	0.50	0.49
Proton (60 MeV)	7.18	6.20	5.08	0.73	1.24	0.40
Proton (100 MeV)	6.46	5.49	5.10	0.75	0.38	0.35
Carbon (300 MeV/u)	8.26	7.81	7.52	1.16	0.55	0.55
Carbon (11.1 MeV/u)	15.21	14.08	11.32	4.51	2.03	1.21

Table 8. Minimum and maximum dendritic length reduction of granule neurons of dentate gyrus following proton radiation and carbon ion beams in 270 Gy D_{TH}.

Particle type (energy beam)	Max reduction length (%)	Min reduction length (%)
Proton (30 MeV)	4.82	0.34
Proton (60 MeV)	4.07	0.29
Proton (100 MeV)	3.60	0.25
Carbon (300 MeV/u)	5.24	0.40
Carbon (11.1 MeV/u)	7.25	0.93

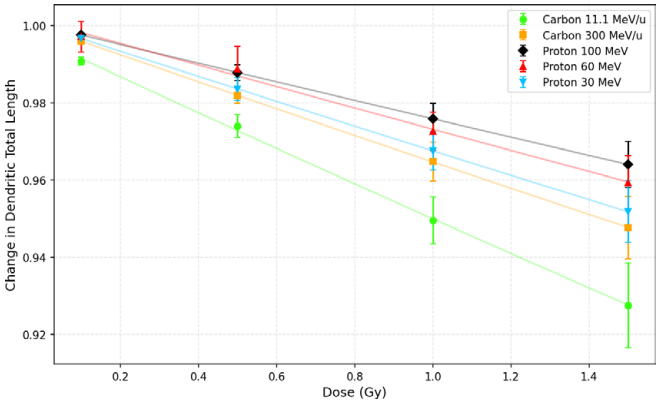

Figure 3. Dose-dependent dendritic damage induced by proton radiation and carbon ion beams on granule neurons in 270 Gy D_{TH}.

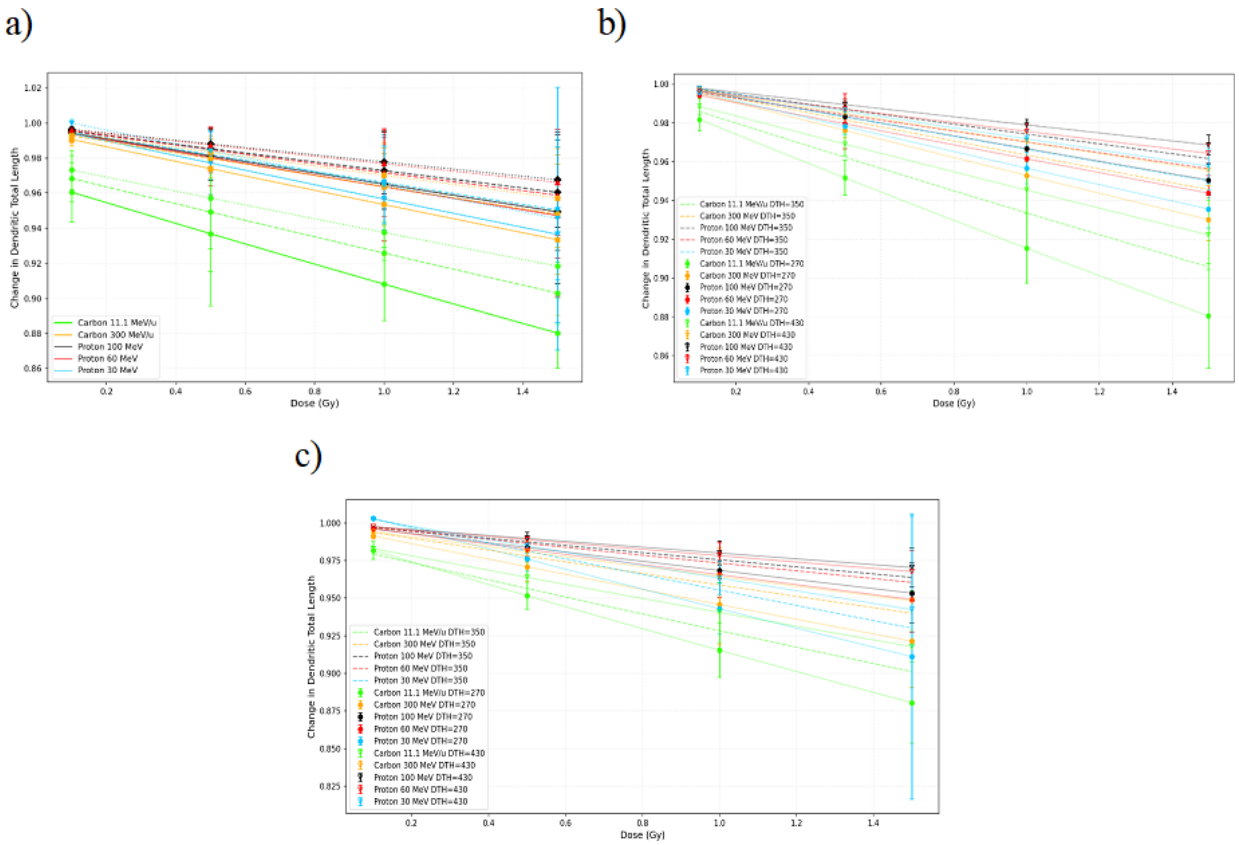

Figure 4. Dose-dependent damage induced by proton radiation and carbon ion beams on apical dendrites of CA1 (a), CA2 (b) and CA3 (c) pyramidal neurons in various D_{TH} values (270, 350 and 430 Gy). Solid, dashed and dotted lines represent dendritic length reduction in the D_{TH} values of 270 Gy, 350 Gy and 430 Gy, respectively.

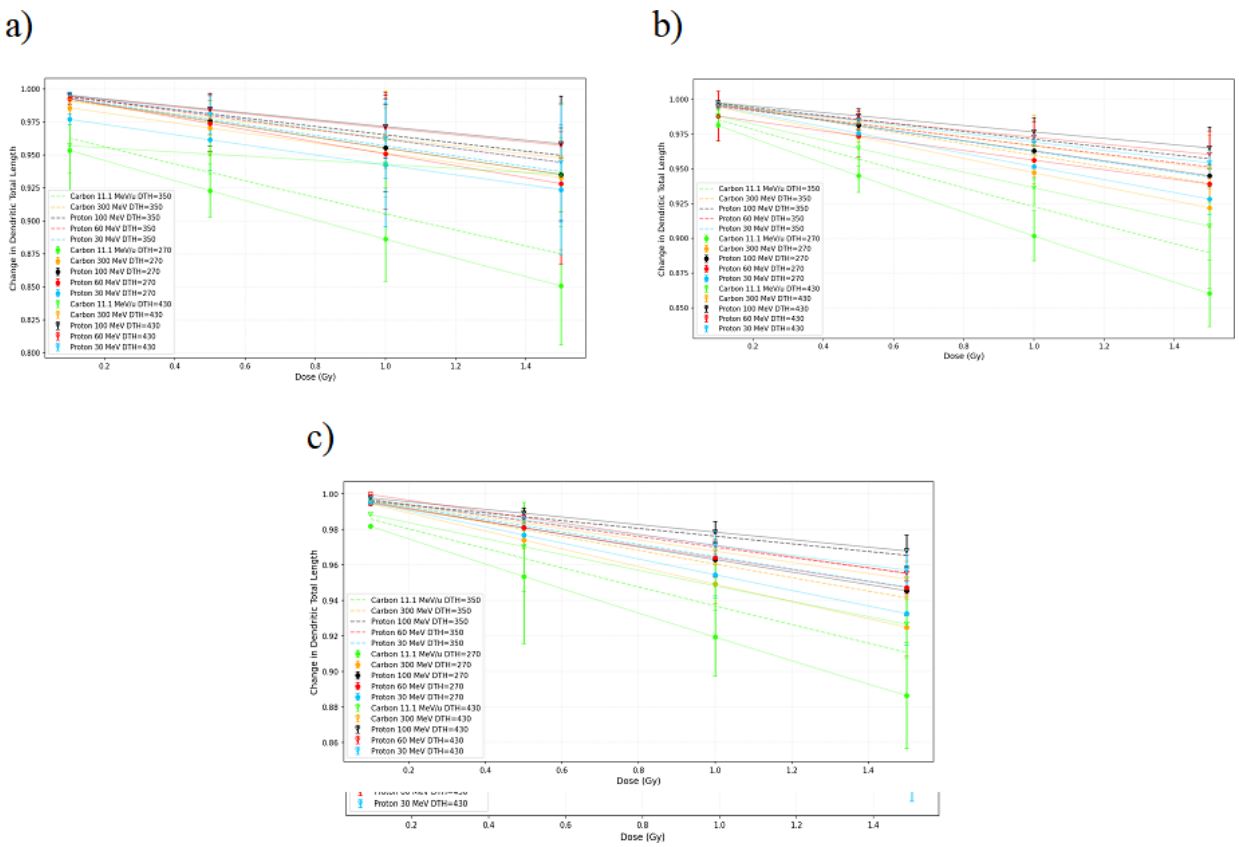

Figure 5. Dose-dependent damage induced by proton radiation and carbon ion beams on basal dendrites of CA1 (a), CA2 (b) and CA3 (c) pyramidal neurons in various D_{TH} values (270, 350 and 430 Gy). Solid, dashed and dotted lines represent dendritic length reduction in the D_{TH} values of 270 Gy, 350 Gy and 430 Gy, respectively.

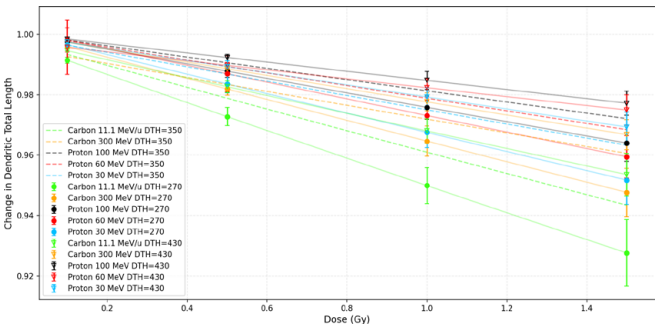

Figure 6. Dose-dependent dendritic damage induced by proton radiation and carbon ion beams on granule neurons in various D_{TH} values (270, 350 and 430 Gy). Solid, dashed and dotted lines represent dendritic length reduction in the D_{TH} values of 270 Gy, 350 Gy and 430 Gy, respectively.

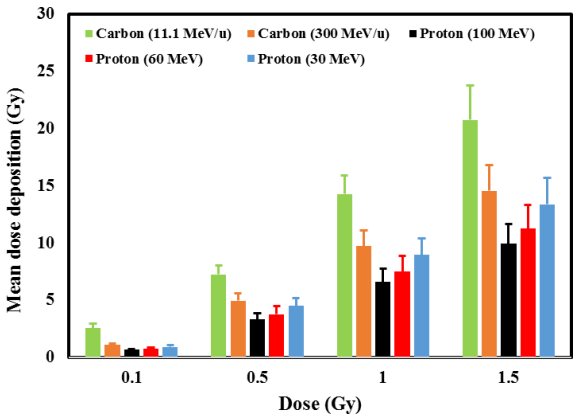

Figure 9. Total dose deposition following proton radiation and carbon ion beams in granule neurons in 270 Gy D_{TH}.

Absorbed dose distribution inside a targeted neuron

The mean dose deposition in different dose values (0.1, 0.5, 1.0, and 1.5 Gy) for apical and basal dendrites of pyramidal neurons and dendrites of dentate granule neurons of hippocampus are illustrated in **Figures 7**, **8,** and **9**. When the dose value was increased from 0.1 Gy to 1.5 Gy, the mean absorbed dose in dendrites increased. The highest and lowest mean dose deposition belonged to carbon ion beams with 11.1 MeV/u energy and the proton radiation with 100 MeV energy, respectively.

As seen from **Figure 7**, the maximum absorbed dose following the 11.1 MeV/u carbon ions with 0.1 and 1.5 Gy doses was detected for apical dendrites of CA1 region; however, for 300 MeV/u carbon ions there was no much difference in the absorbed dose of the apical dendrites of CA regions, except in the CA3 region that absorbed dose in 1 Gy dose was largest. For proton irradiation, the absorbed dose of apical dendrites was almost the same in all CA regions, except in 1.5 Gy dose for 30 MeV that absorbed dose of CA3 region was highest. **Figure 8** also shows that the maximum and minimum absorbed dose values belonged to CA1 and CA3 regions, respectively. As shown in **Figure 9**, the absorbed dose values of dendrites of dentate granule neurons were lower than the CA regions.

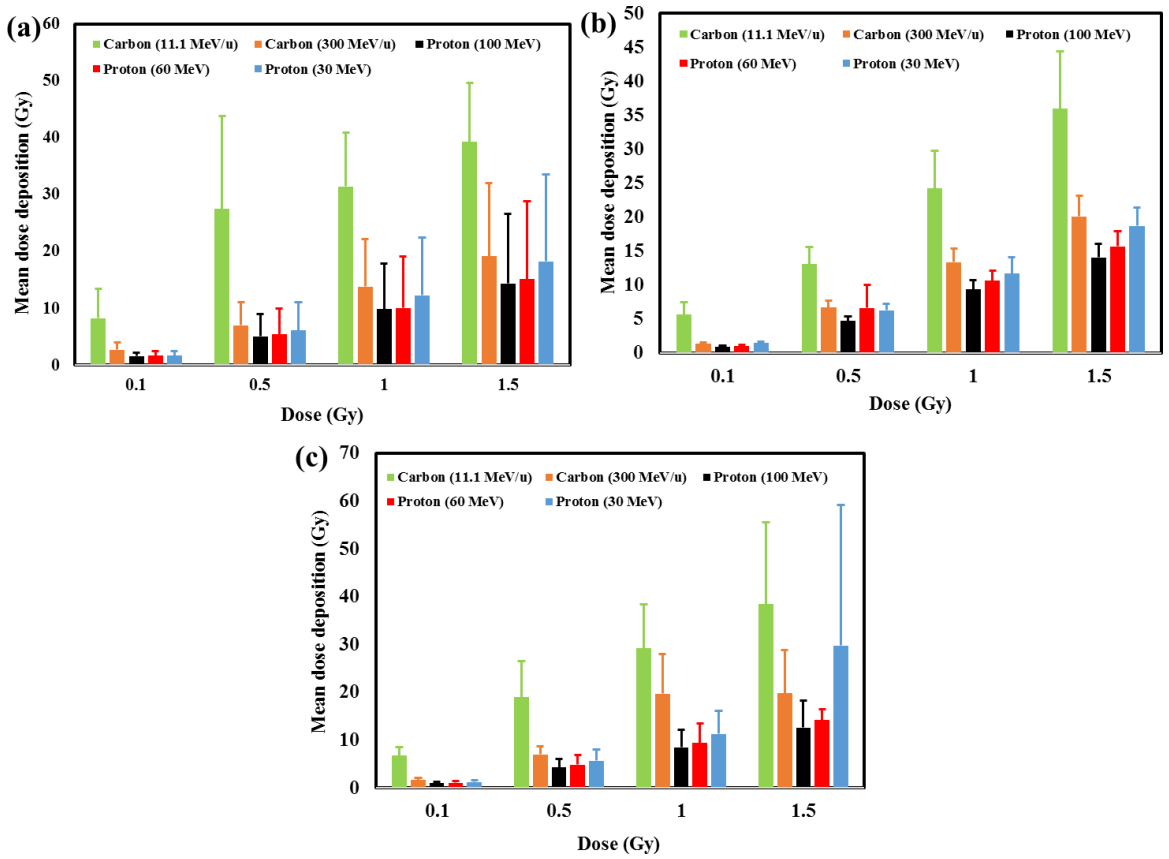

Figure 7. Total dose deposition following proton radiation and carbon ion beams in apical dendrites of CA1 (a), CA2 (b) and CA3 (c) pyramidal neurons in 270 Gy D_{TH}.

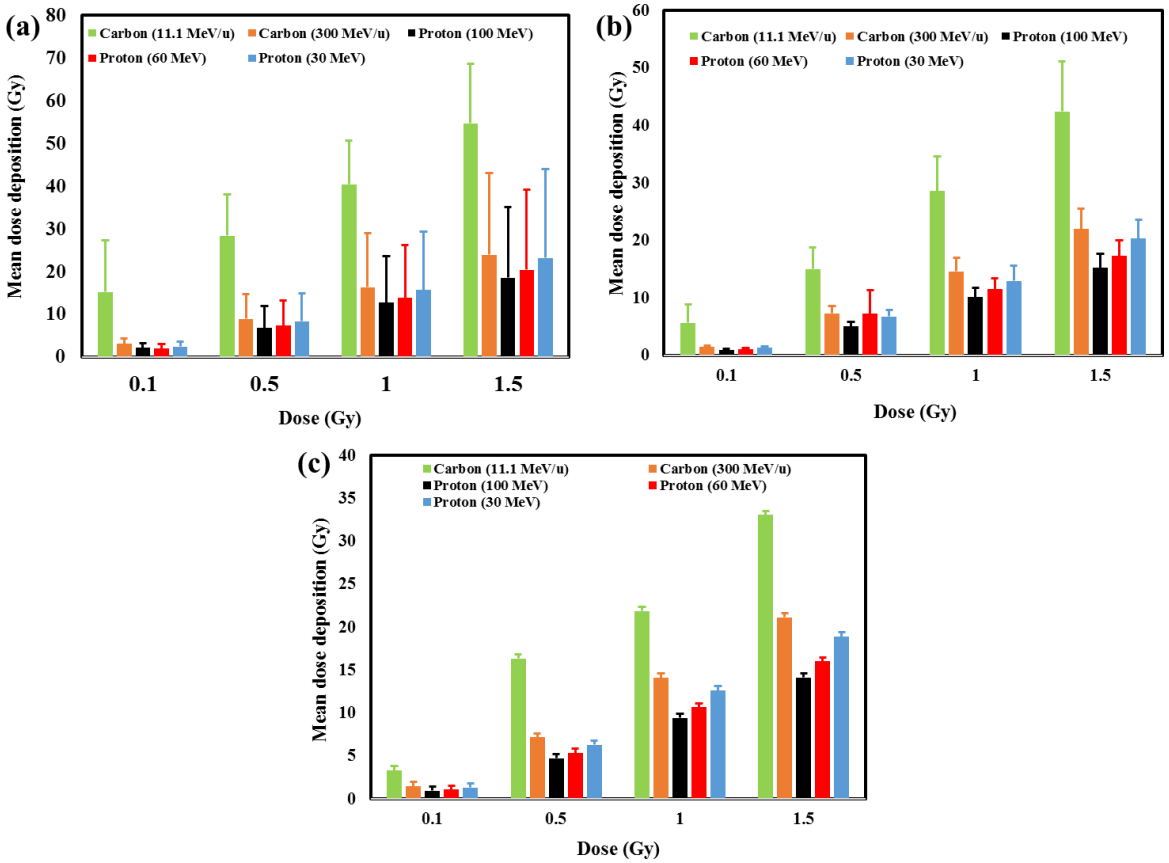

Figure 8. Total dose deposition following proton radiation and carbon ion beams in basal dendrites of CA1 (a), CA2 (b) and CA3 (c) pyramidal neurons in 270 Gy D_{TH}.

Spearman's correlation between morphological characteristics of neurons and the amount of length reduction

Spearman's correlation analysis revealed statistically significant relationships between several morphological characteristics of neurons and the amount of dendritic length reduction (p-value < 0.05). It should be noted that due to the small sample size (number of neurons studied), a non-significant correlation does not necessarily indicate the absence of an actual relationship.

For pyramidal neurons, a larger total dendritic volume was associated with greater reduction in apical dendrite length following carbon ion beams at 11.1 MeV/u for doses of 0.1, 0.5, and 1 Gy (N=13, p-value<0.05; r0.1 Gy=0.72, r0.5 Gy=0.72, r1 Gy=0.67).

The number of apical dendrite branches also showed statistically significant correlations with dendritic length reduction after proton radiation at 30 MeV and 100 MeV and carbon ion radiation at 300 MeV/u (0.1 Gy). Specifically, r=0.62 for 30 MeV protons, r=0.56 for 100 MeV protons, and r=0.68 for carbon ions (N=13, p-value<0.05), indicating that neurons with more apical branches experienced greater length reduction.

Similarly, the number of apical dendrite bifurcations was significantly correlated with apical dendrite shortening under the same radiation conditions (r=0.56 for 30 MeV protons, r=0.68 for 100 MeV protons, r=0.62 for carbon ions; N=13, p-value<0.05).

The total height of apical dendrites also correlated with dendritic reduction following carbon ions at 300 MeV/u for doses of 0.5 and 1 Gy (r0.5 Gy=-0.59, r1 Gy=-0.56; N=13, p-value<0.05).

For basal dendrites, total dendritic volume was inversely correlated with length reduction after proton irradiation at 30 MeV and 60 MeV (0.5, 1, 1.5 Gy) and carbon ions at 300 MeV/u (1 and 1.5 Gy). For example, r0.5 Gy=-0.59, r1 Gy=-0.62, r1.5 Gy=-0.64 for 30 MeV protons, indicating that neurons with larger basal dendritic volume experienced less reduction.

Basal dendrite total height showed similar inverse correlations under carbon ion irradiation at 11.1 MeV/u (0.1, 0.5, 1.5 Gy; r0.1 Gy=-0.69, r1 Gy=-0.73, r1.5 Gy=-0.73; N=13, p-value<0.05).

The overall depth of basal dendrites also correlated significantly with length reduction under proton irradiation (30 MeV: r0.5 Gy=0.56, r1 Gy=0.62, r1.5 Gy=0.64; 60 MeV: r0.5 Gy=0.57, r1 Gy=0.61) and carbon ions (300 MeV/u: r1 Gy=-0.61, r1.5 Gy=-0.61; N=13, p-value<0.05).

For dentate granule neurons, no statistically significant correlations were found between dendritic morphology and length reduction (p-value>0.05), likely due to the small number of neurons simulated. Nonetheless, the lack of significance does not imply the absence of a true relationship.

Discussion

this study, we used the Geant4 Monte Carlo toolkit to estimate the radiation-induced damage in hippocampal neurons caused by proton and carbon ion beams. The hippocampus was chosen because growing experimental evidence highlights its central role in memory and learning, as well as its sensitivity to radiation. It is critical for short- and long-term memory, spatial memory, and navigation[3]. Our findings help establish a connection between radiation-induced changes in pyramidal and dentate granule neurons and potential cognitive deficits.

Previous simulation studies have focused on building highly detailed neuronal models, such as the work by Peter et al. (2022) using TOPAS-nBio, which allowed thousands of in silico realizations of CA1 pyramidal neurons. In contrast, our study concentrated on a smaller, more manageable dataset, simulating the morphology of reconstructed neurons under defined radiation conditions and comparing the resulting morphological changes[6,7,11,19,21]. Despite the limited sample size, the simulations revealed consistent differences across hippocampal regions. While running a larger number of simulations could provide stronger statistical power, it is also very time-consuming. Our results can thus be considered a first step, highlighting patterns that can guide future research.

Comparison with experimental data further supports our findings. Meta-analyses in patients with persistent epilepsy show that basal dendrites of CA1 neurons are particularly vulnerable to loss. Our results **Figures 7-9** align with this, demonstrating higher absorbed doses in CA1 basal dendrites compared to CA2 and CA3. Large CA1 pyramidal neurons were among the most vulnerable, whereas CA2 and CA3 pyramidal neurons and dentate granule cells were more resistant and affected later in Alzheimer's disease progression[13].

Studies on glucocorticoid exposure and restraint stress in mice also support these patterns. Twenty-one days of glucocorticoid injections led to fewer apical dendritic branches and shorter apical dendrites in CA3 neurons, without significantly affecting CA1 or dentate gyrus neurons[22]. Similarly, mice subjected to 21 days of restraint stress (6 hours/day) showed comparable effects in CA3 pyramidal neurons[23]. Our dose distribution results correspond well with these findings, showing higher absorbed doses in apical dendrites of CA3 relative to CA1 and CA2.

Across all figures, dentate granule neurons consistently showed greater resistance to radiation compared to pyramidal neurons. Alkadhi reported that while the DG is largely resilient to various stressors, the CA1 region is particularly vulnerable. Structural differences and variations in the expression of subcellular proteins may explain these distinct responses[9]. Additionally, the DG's potential for neurogenesis, which is limited in CA1 neurons, may contribute to this resilience[24,25], although definitive evidence is still lacking[9].

Variations in the dendritic threshold dose (DTH) affected both single-neuron and population-level morphometric characteristics. Lower DTH values led to more dendritic snips and greater length reduction. Increasing absorbed dose further amplified these effects. Dendritic snips are determined by DTH and the energy deposited in dendritic segments. As shown in **Figures 4-6**, the number of snips at a given absorbed dose was higher for ^{12}C beams than for proton radiation across a range

of DTH values, resulting in greater dendritic length reduction with carbon beams. Reducing DTH increased sensitivity to proton-induced damage, primarily due to the loss of dendritic fragment binding and overall dendritic shortening, which is evident in both pyramidal and dentate granule neurons.

The distribution of energy and dose depends on particle fluence, ion type, and kinetic energy, which are influenced by radiation dose and cell morphology[5]. Higher absorbed doses increased the risk of dendritic injury **Figures 7-9**.

Other non-radiation factors, such as aging[26], excessive glutamate receptor activation[27], and disruptions in calcium homeostasis[28], are also known to shorten hippocampal dendrites. This suggests that dendritic morphology is a general determinant of neuronal vulnerability. Our correlation analysis showed that some morphological features, including total branching and dendritic volume, were significantly associated with dendritic length reduction ($p < 0.05$). Due to the limited number of neurons, non-significant correlations do not necessarily indicate absence of a relationship.

Experimental studies indicate that CA2 pyramidal neurons resemble CA3 neurons in size and packing density and have fewer oblique dendrites compared to CA1 neurons[29,30]. Despite numerous potential pathways leading to cell death, CA2 neurons appear remarkably resistant to various damage mechanisms[31]. Dendritic branches in CA1 neurons are smaller, shorter, and more homogeneous (~13.5 μm) than those in CA2 and CA3 (10–16 μm)[32]. Comparing these findings with our correlation analysis suggests that neurons with more dendritic branches, bifurcations, and higher dendritic density are more vulnerable to radiation damage.

Overall, our results indicate that neuronal morphology is a key factor in determining radiation-induced damage. Alterations in dendritic and spine structure, along with changes in neurotransmitter expression, are well-known contributors to cognitive decline in aging and early neurodegenerative diseases such as Alzheimer's and Parkinson's[33,34]. Many of the effects observed in our study relate to changes in dendritic outgrowth, elongation, branching, number of dendritic endings, and cell body area[35,36]. Both intrinsic and extrinsic factors – including dendritic arborization, synaptogenesis, electrical activity, neuronal maturation and radiation exposure influence these changes[37-47].

Conclusion

In the current study, the dose deposition and dendritic length reduction in pyramidal neurons of CA1, CA2, CA3 and dentate granule neurons of dentate gyrus exposed to ^{12}C ion beams and proton radiation were investigated by the Geant4-DNA toolkit.

By examining the results of the simulation of the morphological characteristics of neurons from different areas of the hippocampus, we found that the morphology of the neurons can be a determining factor for the amount of damage caused by radiation. Neurons with denser dendritic branches will be more vulnerable to radiation

Due to the difference in the morphology of pyramidal and dentate granule neurons, they have different vulnerability to radiation, pyramidal neurons of the CA2 region are more resistant to radiation due to the lower density of dendrites.

Since some of the parameters evaluated in this study (such as inadequate Golgi staining, an intricate structure of a dendritic tree, the long-term nature of the majority of the neurological effects induced by HZE radiation, etc.) cannot be examined experimentally in real neurons, the represented data may be critical for understanding the events that lead to future functional changes in the CNS.

It is problematic to compare the findings of this study with other published studies due to differences in animal models, brain areas, and dose values used in different experiments. However, the findings represented in this study are particularly significant in terms of hadron beam therapy issues. In the case of brain cancers, studying radiation damage to specific neurons could reveal the factors that influence the treatment negative effects. Estimating dose deposition to neural cells surrounding the treated area may be critical for predicting subsequent neuron death processes and the development of cognitive deficits. Finally, because the CNS is one of the most important systems affected by HZE particles, the methodologies discussed in this study may be useful in continuing studies on space radiation risk assessment.

Acknowledgment

The present study was funded by Kashan University of Medical Sciences, Kashan, Iran (with Ethics Code of IR.KAUMS. NUHEPM.REC. 1399. 094).

References

1. Schulz-Ertner D, Tsujii H. Particle Radiation Therapy Using Proton and Heavier Ion Beams. JCO. 2007;25(8):953-964. doi:10.1200/jco.2006.09.7816
2. Olsen DR, Bruland ØS, Frykholm G, Norderhaug IN. Proton therapy – A systematic review of clinical effectiveness. Radiotherapy and Oncology. 2007;83(2):123-132. doi:10.1016/j.radonc.2007.03.001
3. Cucinotta FA, Alp M, Sulzman FM, Wang M. Space radiation risks to the central nervous system. Life Sciences in Space Research. 2014;2:54-69. doi:10.1016/j.lssr.2014.06.003
4. Parihar VK, Allen B, Tran KK, et al. What happens to your brain on the way to Mars. Sci Adv. 2015;1(4). doi:10.1126/sciadv.1400256
5. Batmunkh M, Belov OV, Bayarchimeg L, Lhagva O, Sweilam NH. Estimation of the spatial energy deposition in CA1 pyramidal neurons under exposure to 12C and 56Fe ion beams. Journal of Radiation Research and Applied Sciences. 2015;8(4):498-507. doi:10.1016/j.jrras.2015.05.008

6. Belov OV, Batmunkh M, Incerti S, Lkhagva O. Radiation damage to neuronal cells: Simulating the energy deposition and water radiolysis in a small neural network. Physica Medica. 2016;32(12):1510-1520. doi:10.1016/j.ejmp.2016.11.004
7. Cacao E, Parihar VK, Limoli CL, Cucinotta FA. Stochastic Modeling of Radiation-induced Dendritic Damage on in silico Mouse Hippocampal Neurons. Sci Rep. 2018;8(1). doi:10.1038/s41598-018-23855-9
8. Cucinotta FA, Eliedonna Cacao MA. DETRIMENTS IN NEURON MORPHOLOGY FOLLOWING HEAVY ION IRRADIATION: WHAT'S THE TARGET? Radiation Protection Dosimetry. 2018;183(1-2):69-74. doi:10.1093/rpd/ncy265
9. Alkadhi KA. Cellular and Molecular Differences Between Area CA1 and the Dentate Gyrus of the Hippocampus. Mol Neurobiol. 2019;56(9):6566-6580. doi:10.1007/s12035-019-1541-2
10. Conrad CD, Ortiz JB, Judd JM. Chronic stress and hippocampal dendritic complexity: Methodological and functional considerations. Physiology & Behavior. 2017;178:66-81. doi:10.1016/j.physbeh.2016.11.017
11. Dudek SM, Alexander GM, Farris S. Rediscovering area CA2: unique properties and functions. Nat Rev Neurosci. 2016;17(2):89-102. doi:10.1038/nrn.2015.22
12. Lambert KG, Buckelew SK, Staffiso-Sandoz G, et al. Activity-stress induces atrophy of apical dendrites of hippocampal pyramidal neurons in male rats. Physiology & Behavior. 1998;65(1):43-49. doi:10.1016/s0031-9384(98)00114-0
13. Mrdjen D, Fox EJ, Bukhari SA, Montine KS, Bendall SC, Montine TJ. The basis of cellular and regional vulnerability in Alzheimer's disease. Acta Neuropathol. 2019;138(5):729-749. doi:10.1007/s00401-019-02054-4
14. Vyas A, Mitra R, Shankaranarayana Rao BS, Chattarji S. Chronic Stress Induces Contrasting Patterns of Dendritic Remodeling in Hippocampal and Amygdaloid Neurons. J Neurosci. 2002;22(15):6810-6818. doi:10.1523/jneurosci.22-15-06810.2002
15. Spruston N. Pyramidal neurons: dendritic structure and synaptic integration. Nat Rev Neurosci. 2008;9(3):206-221. doi:10.1038/nrn2286
16. Alp M, Cucinotta FA. Track structure model of microscopic energy deposition by protons and heavy ions in segments of neuronal cell dendrites represented by cylinders or spheres. Life Sciences in Space Research. 2017;13:27-38. doi:10.1016/j.lssr.2017.03.004
17. Tsujii H. Overview of Carbon-ion Radiotherapy. J Phys: Conf Ser. 2017;777:012032. doi:10.1088/1742-6596/777/1/012032
18. Batmunkh M, Bugay A, Bayarchimeg L, Lkhagva O. Radiation Damage to Nervous System: Designing Optimal Models for Realistic Neuron Morphology in Hippocampus. Adam Gh, Buša J, Hnatič M, Podgainy D, eds. EPJ Web Conf. 2018;173:05004. doi:10.1051/epjconf/201817305004
19. Alp M, Cucinotta FA. Biophysics Model of Heavy-Ion Degradation of Neuron Morphology in Mouse Hippocampal Granular Cell Layer Neurons. Radiation Research. 2018;189(3):312-325. doi:10.1667/rr14923.1
20. Spencer RL, Bland ST. Hippocampus and Hippocampal Neurons. Stress: Physiology, Biochemistry, and Pathology. Published online 2019:57-68. doi:10.1016/b978-0-12-813146-6.00005-9
21. Bayarchimeg L, Batmunkh M, Belov O, Lkhagva O. Simulation of Radiation Damage to Neural Cells with the Geant4-DNA Toolkit. Adam Gh, Buša J, Hnatič M, Podgainy D, eds. EPJ Web Conf. 2018;173:05005. doi:10.1051/epjconf/201817305005
22. Woolley CS, Gould E, McEwen BS. Exposure to excess glucocorticoids alters dendritic morphology of adult hippocampal pyramidal neurons. Brain Research. 1990;531(1-2):225-231. doi:10.1016/0006-8993(90)90778-a
23. Watanabe Y, Gould E, McEwen BS. Stress induces atrophy of apical dendrites of hippocampal CA3 pyramidal neurons. Brain Research. 1992;588(2):341-345. doi:10.1016/0006-8993(92)91597-8
24. Ormerod BK, Palmer TD, Caldwell MA. Neurodegeneration and cell replacement. Phil Trans R Soc B. 2007;363(1489):153-170. doi:10.1098/rstb.2006.2018
25. Pawluski JL, Brummelte S, Barha CK, Crozier TM, Galea LAM. Effects of steroid hormones on neurogenesis in the hippocampus of the adult female rodent during the estrous cycle, pregnancy, lactation and aging. Frontiers in Neuroendocrinology. 2009;30(3):343-357. doi:10.1016/j.yfrne.2009.03.007
26. Mattson MP, Magnus T. Ageing and neuronal vulnerability. Nat Rev Neurosci. 2006;7(4):278-294. doi:10.1038/nrn1886
27. Mattson MP. Glutamate and Neurotrophic Factors in Neuronal Plasticity and Disease. Annals of the New York Academy of Sciences. 2008;1144(1):97-112. doi:10.1196/annals.1418.005
28. Mattson MP, Chan SL. Neuronal and glial calcium signaling in Alzheimer's disease. Cell Calcium. 2003;34(4-5):385-397. doi:10.1016/s0143-4160(03)00128-3
29. Ishizuka N, Cowan WM, Amaral DG. A quantitative analysis of the dendritic organization of pyramidal cells in the rat hippocampus. J of Comparative Neurology. 1995;362(1):17-45. doi:10.1002/cne.903620103
30. Lorente de No R. Studies on the structure of the cerebral cortex. II. Continuation of the study of the ammonic system. Journal fur Psychologie und Neurologie. 1934;46:113-177.
31. Dudek SM, Alexander GM, Farris S. Rediscovering area CA2: unique properties and functions. Nat Rev Neurosci. 2016;17(2):89-102. doi:10.1038/nrn.2015.22
32. Cappaert NLM, Van Strien NM, Witter MP. Hippocampal Formation. The Rat Nervous System. Published online 2015:511-573. doi:10.1016/b978-0-12-374245-2.00020-6
33. Dickstein DL, Brautigam H, Stockton SD Jr, Schmeidler J, Hof PR. Changes in dendritic complexity and spine morphology in transgenic mice expressing human wild-type tau. Brain Struct Funct. 2010;214(2-3):161-179. doi:10.1007/s00429-010-0245-1
34. Mufson EJ, Binder L, Counts SE, et al. Mild cognitive impairment: pathology and mechanisms. Acta Neuropathol. 2011;123(1):13-30. doi:10.1007/s00401-011-0884-1
35. Dickstein DL, Weaver CM, Luebke JI, Hof PR. Dendritic spine changes associated with normal aging. Neuroscience. 2013;251:21-32. doi:10.1016/j.neuroscience.2012.09.077
36. Yoshihara Y, De Roo M, Muller D. Dendritic spine formation and stabilization. Current Opinion in Neurobiology. 2009;19(2):146-153. doi:10.1016/j.conb.2009.05.013
37. Chen LY, Rex CS, Pham DT, Lynch G, Gall CM. BDNF Signaling during Learning Is Regionally Differentiated within Hippocampus. J Neurosci. 2010;30(45):15097-15101. doi:10.1523/jneurosci.3549-10.2010
38. Das K. Assessment of PC12 cell differentiation and neurite growth: a comparison of morphological and neurochemical measures. Neurotoxicology and Teratology. 2004;26(3):397-406. doi:10.1016/j.ntt.2004.02.006
39. Thoenen H. The changing scene of neurotrophic factors. Trends in Neurosciences. 1991;14(5):165-170. doi:10.1016/0166-2236(91)90097-e
40. Allen AR, Raber J, Chakraborti A, Sharma S, Fike JR. 56Fe Irradiation Alters Spine Density and Dendritic Complexity in the Mouse Hippocampus. Radiation Research. 2015;184(6):586-594. doi:10.1667/rr14103.1

41. BRIZZEE KR, ORDY JM, KAACK MB, BEAVERS T. Effect of Prenatal Ionizing Radiation on the Visual Cortex and Hippocampus of Newborn Squirrel Monkeys. Journal of Neuropathology and Experimental Neurology. 1980;39(5):523-540. doi:10.1097/00005072-198009000-00002

42. Chakraborti A, Allen A, Allen B, Rosi S, Fike JR. Cranial Irradiation Alters Dendritic Spine Density and Morphology in the Hippocampus. Tofilon PJ, ed. PLoS ONE. 2012;7(7):e40844. doi:10.1371/journal.pone.0040844

43. Chmielewski NN, Caressi C, Giedzinski E, Parihar VK, Limoli CL. Contrasting the effects of proton irradiation on dendritic complexity of subiculum neurons in wild type and MCAT mice. Environ and Mol Mutagen. 2016;57(5):364-371. doi:10.1002/em.22006

44. Kovalchuk A, Mychasiuk R, Muhammad A, et al. Profound and Sexually Dimorphic Effects of Clinically-Relevant Low Dose Scatter Irradiation on the Brain and Behavior. Front Behav Neurosci. 2016;10. doi:10.3389/fnbeh.2016.00084

45. Parihar VK, Limoli CL. Cranial irradiation compromises neuronal architecture in the hippocampus. Proc Natl Acad Sci USA. 2013;110(31):12822-12827. doi:10.1073/pnas.1307301110

46. Parihar VK, Pasha J, Tran KK, Craver BM, Acharya MM, Limoli CL. Persistent changes in neuronal structure and synaptic plasticity caused by proton irradiation. Brain Struct Funct. 2014;220(2):1161-1171. doi:10.1007/s00429-014-0709-9

47. Shirai K, Mizui T, Suzuki Y, et al. X Irradiation Changes Dendritic Spine Morphology and Density through Reduction of Cytoskeletal Proteins in Mature Neurons. Radiation Research. 2013;179(6):630-636. doi:10.1667/rr3098.1